Direct vs Indirect Mechanisms for Electron Injection in Dye-Sensitized Solar Cells

ARTICLE *in* THE JOURNAL OF PHYSICAL CHEMISTRY C · APRIL 2011

Impact Factor: 4.77 · DOI: 10.1021/jp201233y

5 AUTHORS, INCLUDING:

Rocío Sánchez-de-Armas
Uppsala University
14 PUBLICATIONS **354** CITATIONS
SEE PROFILE

Miguel San-Miguel
University of Campinas
53 PUBLICATIONS **749** CITATIONS
SEE PROFILE

Javier Fdez Sanz
Universidad de Sevilla
62 PUBLICATIONS **1,635** CITATIONS
SEE PROFILE

THE JOURNAL OF PHYSICAL CHEMISTRY C

ARTICLE

pubs.acs.org/JPCC

Direct vs Indirect Mechanisms for Electron Injection in Dye-Sensitized Solar Cells

Rocío Sánchez-de-Armas,* Jaime Oviedo, Miguel Ángel San Miguel, and Javier Fdez. Sanz

Department of Physical Chemistry, University of Seville, Seville 41012, Spain

ABSTRACT: Dye-sensitized solar cells based on organic dyes have attracted considerable attention in recent years. These dyes present important differences in geometry and electronic structure, and diverse mechanisms for electronic injection into semiconductor conduction band have been reported. In this work, the electronic structure and the optical response of several dyes, free and bound to TiO_2, have been analyzed and compared using time-dependent density functional theory (TD-DFT) performing calculations both in real time and frequency domains. The aim is to illustrate which aspects of each sensitizer produce different electron injection mechanisms. From the analysis it is concluded that for adsorbed NKX-2311, a coumarin based dye, the photoexcitation occurs toward an orbital mainly localized on the molecule, so this molecule is classified as a type I sensitizer, which follows an indirect mechanism for electron injection. In contrast, catechol and 2,3-naphthalenediol are type II sensitizers and follow a direct mechanism for injecting electrons into the TiO_2 conduction band. In this case, a new band appears in the spectrum, which corresponds to a photoexcitation from states fully localized on the dye to states mainly localized on the cluster but with appreciable dye contribution. NKX-2311 and catechol show limit behaviors. Nevertheless, intermediate ones are also possible. As we move in the sequence catechol, 2,3-naphthalenediol, C343, alizarin, and NKX-2311, we pass progressively from a purely direct injection mechanism to a purely indirect injection mechanism. This is related to the relative position of the molecule LUMO energy to the edge of the semiconductor conduction band.

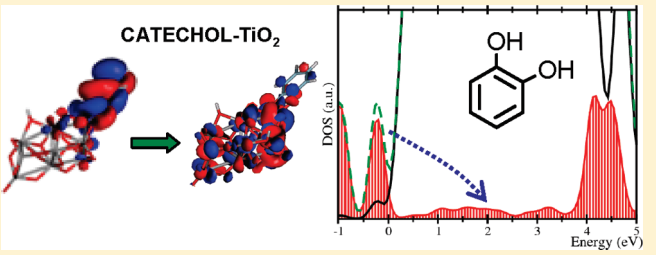

1. INTRODUCTION

Dye-sensitized solar cells (DSSC) have attracted considerable attention in recent years.[1−3] They are based on transition metal derivatives or organic dye molecules that are adsorbed on a semiconductor, generally a metal oxide such as TiO_2. The photochemical properties of different sensitizers have extensively been investigated, in an attempt to design dyes with maximal visible light absorption coupled to long-lived excited states. However, major effort is still invested in both developing new ones and finding optimal working conditions to improve the photon-to-current conversion efficiencies. Ruthenium dyes are the most efficient sensitizers in DSSCs by now, although they have some disadvantages. Molecular modification of these dyes is an arduous task due to their complicated synthesis routes, and the materials involved in the synthesis procedures are rather expensive. In contrast, organic dyes have a much lower cost and their molecular design is more convenient and easier. They have large absorption coefficients due to intramolecular $\Pi \rightarrow \Pi^*$ transitions, and there are no concerns about limited resources, because they do not contain noble metals such as Ru.[4,5]

A key process in the operation of this kind of devices is the charge injection from the dye molecule adsorbed on the nanoparticle surface to the conduction band states of the semiconductor. The injection rate has been found to depend on the electronic properties of both the dye and the semiconductor, as well as the distance between them.[6] The DSSCs can be classified into two types, depending on the electron injection mechanism from the dye to the semiconductor. The first mechanism (type I) involves photoexcitation to a dye excited state, from which an electron is transferred to the solid. The second (type II) is a direct mechanism, a "one-step" electron injection from the ground state of the dye to the conduction band of the semiconductor. The direct injection mechanism is related to a new charge-transfer band that appears in the absorption spectrum of the dye upon adsorption, whereas no new bands are seen in the spectrum in the case of the indirect mechanism.[2,7]

The type I mechanism should result in a more efficient electron transfer to the semiconductor conduction band, but the back electron transfer process could also be easy. In contrast, the indirect mechanism is usually characterized by a lower efficiency of the electron injection, but the back electron transfer is hindered due to an energy barrier.[8] Recently, the existence of intermediate regimes between pure indirect and direct injection mechanisms has been proposed. It has even been shown that the same dye can present type I or II charge injection mechanisms upon varying the dye conjugation in the anchoring group.[9]

Two representative organic sensitizers of types I and II are alizarin and catechol, respectively. Both dyes have extensively been studied by experimental and theoretical methods, since they have simple molecular structures, low cost of fabrication, and high photon-to-current conversion efficiencies.[2,6,7,10−15]

Received: February 7, 2011
Revised: April 15, 2011
Published: May 17, 2011

The experimental electronic absorption spectrum for free alizarin shows a low-energy band centered at 2.88 eV (431 nm). That is red-shifted about 0.4 eV upon adsorption on TiO_2, appearing at 2.47 eV (503 nm),[10] which is characteristic of an indirect mechanism. In contrast, catechol adsorbed spectra exhibit a band at 4.70 eV (270 nm), also observed in free catechol molecule spectrum,[16] and a new wide band centered at 3.2 eV (380−390 nm) and extending farther into the visible range with an onset at 2.0 eV (600 nm).[17−19] This is characteristic of a direct injection mechanism (type II), where there is excitation from the dye ground state to the semiconductor conduction band.[20]

Theoretical methods are a powerful tool for molecular design, and conclusions drawn from calculations are valuable guidelines for synthesis of new efficient dyes.[21] In order to model the electronic spectrum of organic dyes time-dependent density functional theory (TD-DFT) has been used. Alizarin and catechol molecules are two of the smallest sensitizer molecules and that makes them good systems to be theoretically investigated.[22,23] Although it is known that TDDFT can significantly underestimate the energies of long-range charge transfer states, that is not the case with the present calculation, in which the photoexcited state shows a moderate and relatively short-ranged charge transfer.[6] Most of previous theoretical works are able to qualitatively show the main features of experimental spectra, and the effect of bonding alizarin to the surface, but, due to the high computational cost of conventional frequency domain TD-DFT implementation, they are limited in size and make it difficult to fully assess the role of the electronic delocalization into the clusters.[10−12]

In recent works we have studied the structural and electronic properties of both dyes supported on several TiO_2 clusters with different sizes.[24,25] From these works it is shown that, although a minimal model can account for the qualitative features of the spectra, it might be too limited in describing the electronic structure of the system, which is essential in describing the dynamics of the electron transfer.

In this work we have extended the comparison to other dyes with the aim of studying the electronic injection mechanism more in depth and generalize the main differences between the two mechanisms. We have also considered the possibility of intermediate regimes between purely indirect and direct injection mechanisms. We have studied five organic dyes of growing size: catechol; 2,3-naphthalenediol;[8] alizarin; and two coumarin based dyes, C343[26−28] and NKX-2311.[29,30] Their structures are shown in Figure 1.

We follow a protocol consisting of two stages, described in detail in a previous work.[24] First, we study the geometries and electronic structures in the electronic ground state of the free organic dyes and the dyes adsorbed on a TiO_2 cluster. Second, we explore the optical response of the different structures using TD-DFT. These calculations are performed in a complementary way through the frequency domain mode and the real time propagation within the adiabatic approximation with a basis set of localized orbitals. Both TD-DFT implementations reach similar results, providing the basis sets and the exchange-correlation functionals are similar.[24] From the analysis of the main contributions to the bands in the spectra, some helpful insights can be drawn to understand the reasons why each sensitizer follows a different electron injection mechanism.

2. COMPUTATIONAL METHODS

In this study, two complementary sets of calculations have been carried out:

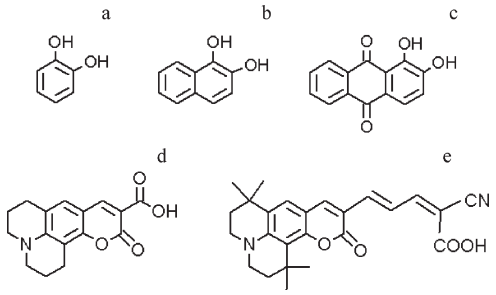

Figure 1. Dye structures: (a) catechol, (b) 2,3-naphthalenediol, (c) alizarin, (d) C343, and (e) NKX-2311.

(1) DFT geometry optimizations have been done by using the PBE generalized gradient approach functional[31] together with norm-conserving pseudopotentials[32] in the fully non-local Kleinman−Bylander[33] form and an auxiliary real-space grid equivalent to a plane-wave cutoff of 130 Ry. A nonstandard DZP basis set of natural atomic orbitals (NAOs) constructed from the eigenstates of the atomic pseudopotential was used.[34−36] The optical response was then computed using real time TD-DFT (time domain) simulations within the SIESTA implementation.[37−39] We consider as an initial state a bound system in a finite electric field of 0.1 V/Å. Each system was allowed to evolve during 60 fs with a time step of 1.5×10^{-3} fs.

(2) Additionally, linear response (LR) frequency domain calculations were performed in the gas phase using the PBE functional and the 6-31G** basis set. The optical spectra were simulated by frequency domain TD-DFT using Gaussian 03.[40] Over 400 singlet transitions were needed in selected calculations.

There are some advantages associated with the real-time TD-DFT formulation: all the possible excitations are generated at the same time, so the spectra is obtained in a wide range of energy; the implementation is relatively simple, and although the computational cost is not cheap for small systems, it becomes competitive with traditional methods as the system size increases. However, the main disadvantage is that it is not possible to characterize the nature of the different transitions, because the optical response is obtained from the analysis of the electronic dipole moment, where the information from the wave functions is integrated. For this reason, the combination with frequency domain TD-DFT is very interesting. In previous work[24,25] we performed real-time calculations with clusters as large as $(TiO_2)_{38}$ and demonstrated that $(TiO_2)_9$ is large enough to reproduce adequately the electronic absorption spectra of the dye−TiO_2 systems.[24] The $(TiO_2)_9$ cluster is affordable from frequency domain TD-DFT calculations, which allows for a full analysis of the spectra.

In a previous work, the effect of the functional and the solvent has been tested for small organic dyes (alizarin and catechol).[24] Conclusions for these works have been extrapolated here for other dyes, which have similar structures. We have done the frequency domain TD-DFT calculations for the free and adsorbed dye using PBE and B3LYP and with and without solvent effects (PCM model). The functional choice is a key parameter when calculating the electronic spectra. The position of the main peak is shifted to higher energies when passing from the PBE to the B3LYP functional. Compared to the experimental spectra, the B3LYP functional gives better results for alizarin while PBE

Table 1. Lowest Band Energies (eV) for Free and Adsorbed Dyes Spectra (from Frequency Domain TD-DFT Calculations and Experimental Values) and Adsorption Energies for the Different Dyes on the $(TiO_2)_9$ Cluster

	free dye (eV)		adsorbed dye (eV)		
dye	calcd	expt	calcd	expt	E_{ads} (eV)
catechol	4.76	4.51	1.2−3.2	1.2−3.2	−1.82
2,3-naphthalenediol	3.92		1.2−3.2	1.2−3.2	−1.81
alizarin	2.67	2.88	2.39	2.47	−0.90
C343	2.96	2.81	2.81	2.71	−1.63
NXX-2311	2.30	2.46	2.17	2.50	−0.81

values are better for catechol. Since there is not a clear choice, we have performed calculations with the PBE functional, which allows for an easier comparison between real-time and frequency calculations. The inclusion of solvent effects through a PCM model tends to reduce the excitation energies (about 0.2−0.3 eV), the red shift being more important for alizarin than for catechol. An extended description of solvent and functional influence is shown in refs 24 and 25.

The computational methodology has been applied to free dyes (catechol, 2,3-naphthalenediol, alizarin, C343, and NKX-2311) and each dye adsorbed on a $(TiO_2)_9$ cluster. The starting geometry for this cluster was taken from the literature.[41,42] It was obtained via geometry optimization of the originally spherical shape, resulting in a compact structure with only 4-fold coordinated Ti atoms and with one terminal Ti−O bond.

All the studied dyes can adsorb to the TiO_2 surface through two oxygen atoms (from hydroxyl groups or from the carboxylic group), and several adsorption configurations are possible, including molecular or dissociative processes.

All previous theoretical work uses a bidentate chelating adsorption mode for alizarin.[24] For catechol, it has been proved that this adsorption mode is also more stable than molecular and monodentate mode, and furthermore, this adsorption mode produces an optimal coupling in the dye−cluster complex that makes the electron injection more efficient.[25] There are no theoretical results of coumarin dyes adsorbed on TiO_2. FTIR spectra show the presence of carboxilate ion after adsorption, which indicates that the deprotonation of the COOH group takes place on the TiO_2 surface.[43] Nevertheless, there is some controversy about which dissociated adsorption mode is the most favorable in this case. We have tested that the system is more stable when the two dye oxygen atoms are bound to the same Ti atom of the cluster.

In this work the dyes have been adsorbed completely dissociated, forming a bidentate bridging structure with one surface titanium atom. In all cases, to keep the system electroneutral, the detached hydrogen atoms have been added to the farthest two-folded O atoms in the cluster. In Table 1 the adsorption energies for the different dyes on the $(TiO_2)_9$ clusters are shown. Adsorption energies are larger for catechol and 2,3-naphthalenediol and smaller for NKX-2311. These energies might be related to the electron injection mechanism.

3. RESULTS AND DISCUSSION

We start this section by analyzing the electronic absorption spectra and the electronic structures of free dyes. The simulated spectra from real-time TD-DFT calculations are shown in Figure 2

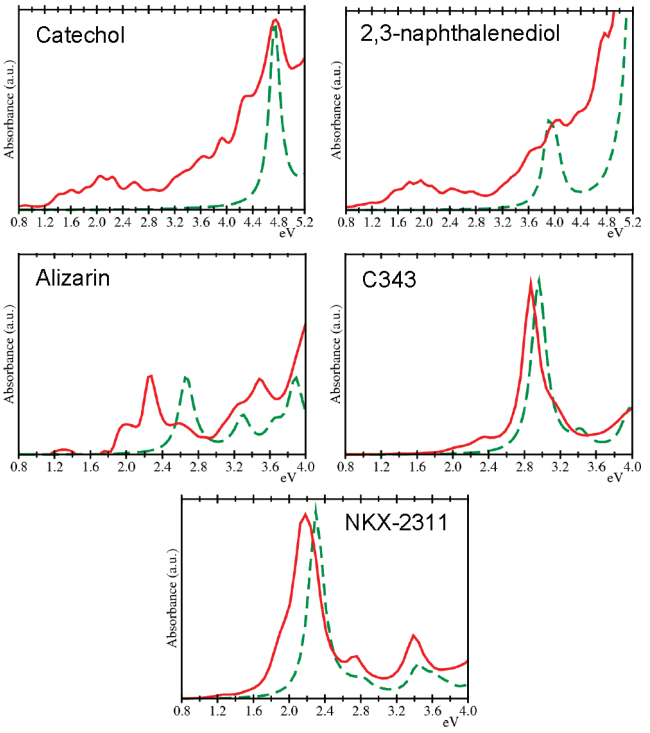

Figure 2. Real-time TD-DFT calculated spectra for free dyes (dashed line) and dyes adsorbed on a $(TiO_2)_9$ cluster (full line).

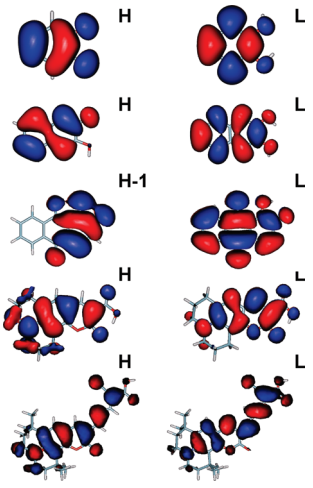

Figure 3. Occupied and virtual molecular orbitals responsible for the first band in the electronic absorption spectrum of free dyes. From top to bottom: catechol, 2,3-naphthalenediol, alizarin, C343, and NKX-2311. H stands for HOMO and L stands for LUMO.

(dashed line). The first band in the spectra of isolated dyes red-shifts while extending the π electron system (Table 1). The most intense contribution to the lowest energy band comes from an excitation from the HOMO to the LUMO orbital, except for alizarin. For this dye, the first band comes from an excitation from the HOMO−1 to the LUMO orbital. These frontier orbitals are represented in Figure 3. For catechol and 2,3-naphthalenediol, HOMO orbital is a π orbital delocalized over the whole molecule. Alizarin HOMO−1 is a π orbital localized over the hydroxyl part of the molecule in which the lone electron pairs of the hydroxyl and quinone oxygens are important contributors. Finally, C343

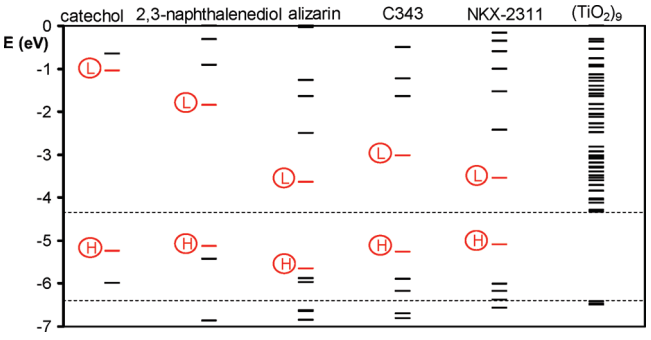

Figure 4. Molecular orbital energies for the ground state. The free dyes, from left to right: catechol, 2,3-naphthalenediol, alizarin, C343, and NKX-2311. In the last column orbital energies for $(TiO_2)_9$ cluster have been included. H stands for HOMO and L stands for LUMO.

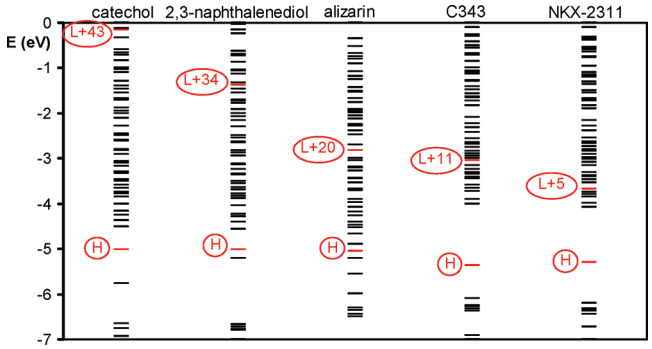

Figure 5. Molecular orbital energies for the ground state. The adsorbed dyes, from left to right: catechol, 2,3-naphthalenediol, alizarin, C343, and NKX-2311. For each dye we have marked the HOMO orbital (H) and the orbital that corresponds to the LUMO of the free molecule. This orbital is more stable as we move in the series: catechol, 2,3-naphthalenediol, alizarin, C343, and NKX-2311.

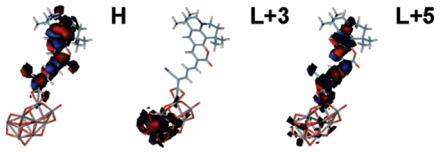

Figure 6. Selected occupied and virtual molecular orbitals of adsorbed NKX-2311. There is very little mixing between cluster and dye orbitals. In general, orbitals are either completely localized on the cluster (like LUMO+3) or completely localized on the dye (like HOMO or LUMO+5). LUMO+5 orbital (LUMO*) contributes to every excitation with considerable intensity in the main band of adsorbed C343 spectra.

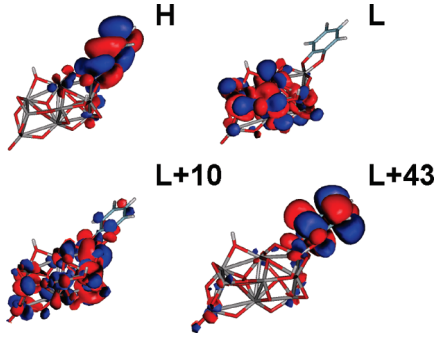

Figure 7. Selected occupied and virtual molecular orbitals of adsorbed catechol. Orbitals from LUMO to LUMO+5 are completely localized on the cluster and they do not contribute in the electronic spectra. In all excitations with considerable intensity in the first band of the spectra, at least one orbital with dye contribution is involved, such as LUMO+10. LUMO+43 (LUMO*) is involved in the excitations that contributes to the second band of the spectra (at 4.76 eV). The orbital scheme is very similar for adsorbed 2,3-naphthalenediol.

and NXK-2311 HOMOs are also π orbitals delocalized over the whole molecule, but with more contribution of coumarin skeleton, which acts as an electron donor. In all cases, the LUMO is a π orbital delocalized over the whole dye, but in the case of NKX-2311, it has a large contribution of cyanoacrilic acid and polymethine chain. Calculated spectra are in good agreement with experimental measurements (Table 1).

In Figure 4 the computed Kohn−Sham orbital energies for free dyes have been represented. In that figure the computed orbital energies for isolated $(TiO_2)_9$ cluster have also been included. For all free dyes the HOMO orbital is located within the cluster band gap and the LUMO orbital is located within the cluster conduction band. These are two requirements that a dye should fulfill to be used as a DSSC sensitizer.[3] Nevertheless, catechol and 2,3-naphthalenediol LUMOs are higher in energy, being placed well into the semiconductor conduction band, while for alizarin, C343, and NKX-2311 the LUMO is more stable, being placed close to the lower edge of the conduction band. Therefore, for catechol and 2,3-naphthalenediol there are a higher number of cluster orbitals located between dye HOMO and LUMO orbitals. The energy gap between HOMO and LUMO orbitals for the different dyes is in agreement with the calculated excitation energies order.

As a result of their different geometries and electronic structures, these dyes present different behaviors after binding to TiO_2. The simulated spectra from real-time TD-DFT calculations for adsorbed dyes are shown in Figure 2 (full line). Bonding NKX-2311 to a titania cluster induces a red-shift (about 0.2 eV) and a slight widening of the lowest energy band. In contrast, catechol and 2,3-naphthalenediol spectra show a new wide band at low energy when the dye is adsorbed to TiO_2, while bands of free molecule spectrum remain almost unaltered. These two behaviors are characteristic of electron injection mechanisms type I and II, respectively. Nevertheless, alizarin and C343 present an intermediate behavior after adsorption. The first band in the adsorbed dye spectrum red-shifts (about 0.3 eV for alizarin and about 0.15 eV for C343) with respect to the spectrum of the free dye and a small new band appears at low energies. In order to understand the differences between these sensitizers, we have analyzed and compared the electronic structure and the main excitations of the spectra of adsorbed dyes.

After binding to titanium there is a redistribution of energy levels. In Figure 5 the computed Kohn−Sham orbital energies for adsorbed dyes have been represented. For the five adsorbed systems, the last occupied orbitals are completely localized on the dye, while first virtual orbitals are completely localized on the cluster. These orbitals are represented in Figures 6−9. The HOMO orbital is, for every adsorbed system, very similar to the same orbital of the free dye. The orbital that corresponds to the LUMO in the free molecule is more stable as we move in the series catechol, 2,3-naphthalenediol, alizarin, C343, and NKX-2311. It corresponds to LUMO+43 for adsorbed catechol, LUMO+34 for adsorbed 2,3-naphthalenediol, LUMO+20 for

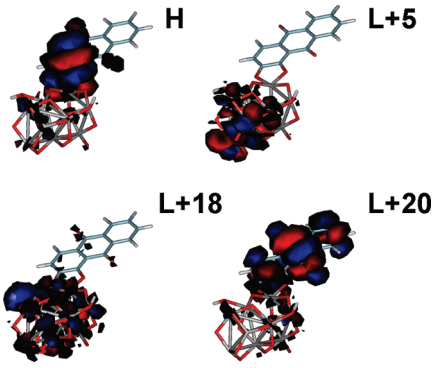

Figure 8. Selected frontier occupied and virtual molecular orbitals of adsorbed alizarin: HOMO, LUMO+5, LUMO+18, and LUMO+20. LUMO+5 does not participate in the electronic spectra because its overlap with the occupied orbitals is negligible. LUMO+20 (LUMO*) is one of the virtual orbitals that contributes most to the main band of absorption spectrum, and LUMO+18 is one of the virtual orbitals implicated in the small band at low energy.

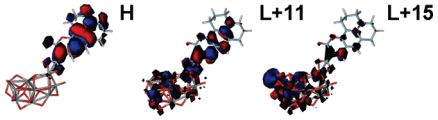

Figure 9. Selected frontier occupied and virtual molecular orbitals of adsorbed C343: HOMO, LUMO+11, and LUMO+15. LUMO+11 is one of the virtual orbitals that contributes most to the main band of absorption spectrum, and LUMO+15 is one of the virtual orbitals implicated in the small shoulder at low energy.

alizarin, LUMO+11 for C343, and LUMO+5 for NKX-2311. In all cases, these orbitals have some contribution from the cluster. For all adsorbed dyes, this orbital plays a crucial role in the electronic absorption spectrum, and we will name it LUMO*. It is interesting to analyze the changes in HOMO and LUMO* energies after adsorption. Catechol, 2,3-naphthalenediol, and alizarin bind to the cluster through the same anchor groups: two hydroxyl groups. For these adsorbed dyes, the HOMO orbital has considerable contribution from the titanium cluster atoms closest to the dye, and both HOMO and LUMO orbitals suffer a destabilization after adsorption. This destabilization is more important for LUMO orbital, resulting in an increase of the HOMO−LUMO* energy gap related to the HOMO−LUMO energy gap for isolated dyes. This increase is a maximum for catechol (0.60 eV) and smaller for 2,3-naphthalenediol (0.33 eV) and alizarin (0.20 eV). In contrast, for C343 and NKX-2311 HOMO orbital stabilizes after adsorption (0.10 and 0.18 eV, respectively). This two dyes bind to the cluster through a different anchor group, a carboxylate group. In these cases, there is no contribution of the cluster in HOMO orbitals. The C343 LUMO remains in the same position after adsorption, while that of NKX-2311 slightly stabilizes (0.13 eV). In consequence, HOMO−LUMO* energy gap slightly increases for C343 (0.10 eV) and it remains unaltered related to the HOMO−LUMO energy gap for free NKX-2311 dye.

The simulated spectra from real-time TD-DFT calculations of adsorbed dyes are shown in Figure 2 (full line). The adsorbed NKX-2311 absorption spectrum shows an intense band with a maximum at 2.2 eV. Several excitations contribute to this band, and each of them corresponds to several pairs of donor and acceptor orbitals (Table 2). All of them are excitations from HOMO orbital to orbitals delocalized over the cluster (LUMO+3, LUMO+15, LUMO+16, LUMO+17) but they have some contribution to the LUMO+5 (or LUMO*) that is an orbital completely localized on the molecule and very similar to the LUMO of free dye (Figure 6). Analyzing the orbitals for adsorbed NKX-2311, it is remarkable that there is very little mixing between cluster and dye orbitals. In general, orbitals are either completely localized on the cluster (like LUMO+3) or completely localized on the dye (like HOMO or LUMO+5).

In contrast, for 2,3-naphthalenediol and catechol the behavior after binding to TiO_2 is completely different from NKX-2311 behavior. For both dyes a new wide band appears in the spectrum after adsorption. This new feature appears at low energy, between 1.2 and 3.2 eV, and it includes numerous excitations (Table 3). The occupied orbitals that contribute most to the first band are for both dyes HOMO and HOMO−1 (Figure 7 top left). They are mainly localized on the dye, and they are very similar to the same orbitals for the free dye. Orbitals from LUMO to LUMO+5 are completely localized on the cluster and they do not have any contribution from the dye (Figure 7 top right). The overlap of these orbitals with the last occupied orbitals is negligible, and consequently, they participate in excitations with negligible intensity. Therefore, these orbitals do not contribute to the first band of the spectra. Orbitals from LUMO+6 to LUMO+30 are the virtual orbitals with most contribution to the first band of the spectra. They are mainly localized on the cluster, and some of them do not have any contribution from the dye. Nevertheless, in all excitations with considerable intensity at least one orbital with dye contribution is involved, such as LUMO+15 for 2,3-naphthalenediol or LUMO+10 for catechol. Most of these orbitals are formed via interaction of d_{z^2} orbitals of Ti atom closest to the dye molecule and p orbitals of dye oxygens (Figure 7 bottom left). This band is associated with a direct photoexcitation from the dye to TiO_2, i.e., by means of a direct mechanism for electron injection. This mechanism requires a strong electronic coupling between semiconductor conduction band and dye molecule, with a proper arrangement of molecular orbitals.[8]

In both cases, above this previously described first band the spectrum shows a second intense one, which coincides with the first band in the free dye spectrum. This band appears at 3.90 eV for adsorbed 2,3-naphthalenediol and is centered at 4.76 eV for adsorbed catechol. Again, this band includes numerous excitations (not included in Table 3). The origin and destiny orbitals of these excitations are very different. Some of them are completely localized on the cluster or on the molecule and some of them are distributed over the whole system. Nevertheless, all excitations with noticeable intensity have a relatively important contribution of the excitation from HOMO to LUMO+34 for 2,3-naphthalenediol or HOMO to LUMO+43 orbital for catechol (Figure 7, bottom right). These virtual orbitals (LUMO+34 and LUMO+43) correspond to LUMO of free dyes, although they have some minor contribution from the cluster. Therefore, this band has the same character as the main band in the free catechol spectrum. Although the orbitals presented in Figure 7 correspond to the catechol−cluster system, the orbital scheme is very similar for adsorbed 2,3-naphthalenediol.

The two behaviors previously described are characteristic of electron injection mechanisms type I and type II, respectively. Nevertheless, alizarin and C343 present an intermediate behavior after adsorption. The main band in calculated adsorbed

Table 2. Assignments of Electronic Excitations for Free and Adsorbed NKX-2311[a]

tyransition energy, eV (excitation number)	oscillator strength	wave function
		Free NKX-2311
2.35	1.0538	H→L (0.56), H−1→L (0.14)
		NKX-2311−$(TiO_2)_9$
2.16 (20)	0.1738	H−1→L+3 (0.49), H→L+15 (−0.41), H→L+5 (−0.16) H→L+13 (0.12), H→L+14 (0.12)
2.23 (22)	0.4445	H→L+16 (0.41), H→L+15 (0.34), H→L+5 (−0.25), H→L+17 (0.20), H→L+13 (0.15), H→L+8 (0.10)
2.27 (23)	0.1768	H→L+16 (−0.55), H→L+17 (0.33), H→L+5 (−0.15), H→L+15 (0.14)
2.33 (25)	0.2141	H→L+17 (0.52), H−2→L+2 (0.30), H→L+5 (0.17), H→L+16 (0.14), H→L+18 (−0.12), H→L+15 (0.11)

[a] Only selected transitions with enough oscillator strength around the main peak are included. H stands for HOMO and L for LUMO.

Table 3. Assignments of Electronic Excitations for Free and Adsorbed 2,3-Naphthalenediol and Catechol[a]

transition energy, eV (excitation number)	oscillator strength	wave function
		Free 2,3-Naphthalenediol
3.88 (1)	0.0438	H→L (0.50), H−1→L (0.30), H→L+1 (0.23), H−1→L+1 (−0.18)
		2,3-Naphthalenediol−$(TiO_2)_9$
1.9973 (30)	0.0365	H−1→L+13 (0.48), H→L+15 (−0.28) H−1→L+14 (−0.23), H−1→L+15 (0.19), H−1→L+10 (0.16), H→L+14 (0.15)
2.2362 (34)	0.0574	H−1→L+15 (0.51), H→L+17 (−0.24) H−1→L+17 (0.15), H→L+18 (0.15) H−1→L+13 (−0.12), H−1→L+16 (−0.12) H−1→L+14 (−0.11), H→L+19 (−0.11) H→L+21 (−0.11)
3.3359 (100)	0.0256	H−3→L+6 (0.40), H→L+30 (0.28) H−1→L+28 (−0.27), H−1→L+26 (0.24) H−1→L+27 (−0.16), H−1→L+30 (0.15) H−1→L+29 (0.13), H→L+32 (0.11) H−8→L+2 (0.10)
		Free Catechol
4.76 (1)	0.0352	H→L (0.58), H−1→L+1 (0.35)
		Cat-2H−$(TiO_2)_9$
2.10 (23)	0.0177	H→L+15 (0.48), H−1→L+7 (−0.31), H−1→L+6 (−0.27), H→L+16 (0.15), H→L+17 (−0.13), H−1→L+8 (0.11)
2.27 (28)	0.0225	H→L+17 (0.54), H−1→L+10 (0.26) H−1→L+8 (−0.14), H→L+15 (0.14) H−2→L+9 (−0.13), H→L+18 (0.12) H→L+16 (−0.11), H−1→L+7 (0.10)
2.39 (31)	0.0324	H−1→L+10 (0.54), H→L+19 (0.23) H→L+20 (0.16), H−1→L+13 (−0.14) H→L+18 (0.14), H→L+17 (−0.12)
3.22 (68)	0.0158	H−1→L+22 (0.36), H→L+28 (0.33) H−1→L+21 (0.30), H→L+27 (0.24), H→L+26 (−0.19), H→L+30 (−0.18) H→L+29 (−0.11)

[a] Only selected transitions with enough oscillator strength around the main peak are included. H stands for HOMO and L for LUMO.

Table 4. Assignments of Electronic Excitations for Free and Adsorbed Alizarin[a]

transition energy, eV (excitation number)	oscillator strength	wave function
		Free Alizarin
2.67 (3)	0.0856	H−1→L (0.63), H−1→L+3 (−0.13), H−3→L+2 (0.11)
		Aliz-2H−$(TiO_2)_9$
1.88 (68)	0.0110	H−1→L+17 (0.47), H−1→L+16 (−0.32), H−6→L (0.29), H→L+18 (0.15) H→L+17 (−0.13), H→L+16 (0.11)
2.31 (100)	0.0310	H→L+22 (0.51), H→L+20 (0.31), H−3→L+11 (0.21), H−2→L+18 (0.16) H−2→L+19 (−0.12)
2.39 (109)	0.0626	H→L+20 (0.39), H−2→L+19 (0.38) H→L+22 (0.26), H−11→L (0.11) H−1→L+22 (−0.10), H−10→L (0.10)

[a] Only selected transitions with enough oscillator strength around the main peak are included. H stands for HOMO and L for LUMO.

alizarin spectrum appears at 2.39 eV (Table 4) and two excitations are the main contributions to it. The occupied orbitals that contribute most are HOMO, HOMO−2, and HOMO−3 (Figure 8 top left). They are all mainly localized on the alizarin, although there is some minor contribution from the Ti atom closest to the molecule. On the other hand, LUMO+20 is one of the main virtual orbitals involved in the excitations. As we can see in Figure 5, this orbital corresponds to the LUMO* orbital. It is therefore localized on the dye and it is very similar to the LUMO in the free molecule (Figure 8, bottom right). Furthermore, the spectrum shows a small band centered at 1.9 eV. It is mainly due to excitations from the HOMO and HOMO−1 (orbitals fully

Table 5. Assignments of Electronic Excitations for Free and Adsorbed Coumarin C343[a]

transition energy, eV (excitation number)	oscillator strength	wave function
		Free C343
3.01	0.3616	H→L (0.59), H−2→L+1 (−0.14), H−2→L (−0.12)
		C343−$(TiO_2)_9$
2.14 (19)	0.0314	H→L+13 (0.48), H→L+11 (0.45) H→L+12 (0.19)
2.28 (22)	0.0228	H→L+15 (0.61), H→L+11 (0.15) H→L+13 (−0.28), H→L+14 (0.13)
2.68 (36)	0.0480	H→L+20 (0.68)
2.80 (45)	0.1553	H−5→L (0.44), H→L+21 (−0.41) H→L+22 (−0.16), H→L+11 (−0.15) H→L+13 (0.14), H→L+15 (0.11) H→L+20 (0.10)
2.85 (50)	0.2731	H→L+21 (−0.44), H→L+22 (0.35) H→L+11 (0.19), H→L+13 (−0.18) H→L+15 (−0.14), H→L+17 (0.11) H→L+20 (−0.11)
3.05 (65)	0.1036	H→L+22 (0.34), H−1→L+15 (0.32) H→L+23 (0.32), H−1→L+16 (0.21) H−1→L+13 (0.14), H→L+11 (−0.11) H→L+13 (0.11), H→L+24 (−0.10)
3.06 (66)	0.0914	H−1→L+16 (0.38), H−1→L+15 (0.35) H→L+22 (−0.23), H−2→L+12 (0.20) H→L+23 (−0.20), H−1→L+17 (0.15) H−1→L+13 (0.12)

[a] Only selected transitions with enough oscillator strength around the main peak are included. H stands for HOMO and L for LUMO.

localized on the dye) to LUMO+16, LUMO+17, and LUMO+18. These virtual orbitals are localized on the cluster, although they have slight contributions from the dye (Figure 8 bottom left). Orbitals from LUMO to LUMO+10 do not participate in the transitions that make up these two bands, because they are totally localized on the side of the cluster furthest from the molecule, so their overlap with the occupied orbitals is negligible (Figure 8, top right).

Finally, the main peak in adsorbed C343 electronic spectrum appears at 2.8 eV. The occupied orbital that contributes most to this band is the HOMO orbital (Figure 9, left). The virtual orbitals with the most contribution are LUMO+11, LUMO+12, LUMO+13, LUMO+15, LUMO+16, LUMO+21, and LUMO+22 (Table 5). LUMO+11 and LUMO+13 are orbitals delocalized over the whole system, while the rest of the orbitals are localized on the cluster and have only slight contributions from the dye (Figure 9 center). In all excitations with considerable intensity, at least one orbital with dye contribution (LUMO+11 or LUMO+13) is involved. Moreover, this main band in adsorbed C343 spectrum presents a small shoulder at low energy (2.1−2.6 eV). The main contributions to this shoulder are excitations from the HOMO to orbitals delocalized over the whole cluster, but with contribution of the dye, like LUMO+15 (Figure 9 right). In consequence, this shoulder has some charge transfer character. For this adsorbed dye more mixing between dye and cluster orbitals than in the case of NKX-2311 is observed. Analyzing the electronic absorption spectra of adsorbed dyes, we can assign the main band in the spectra of adsorbed alizarin and C343 dyes to an indirect electron injection from the last occupied orbitals to an orbital that is very similar to the LUMO of isolated dye, and we can assign the small band at low energies to a direct electron injection into the semiconductor conduction band. Alizarin and C343 represent the intermediate behavior in which both injection regimes are present. The presence of both mechanisms could be the reason why different injection rates have been reported for alizarin−TiO_2 systems.[23]

The match between the dye electronic structure relative to the band structure of the semiconductor has been shown to determine the charge transfer mechanism of the solar cell. A shift in the electronic structure of the semiconductor does not change the order in which the molecules behave; i.e., the NKX-2311 is always more type I-like and catechol is more type II-like. This is a robust conclusion from our work. However, it is worth mentioning that if the semiconductor LUMO lays higher in energy, relative to the molecule LUMO, the direct transfer mechanism would be hindered. This could be dependent on the particular technical parameters (i.e., the use of nonhybrid exchange-correlation potentials tends to underestimate the HOMO−LUMO gap).

To finish the comparison, the partial and total densities of states for adsorbed dyes have been calculated, and they are shown in Figure 10. The diagrams have been shifted to set the Fermi level as the zero energy. For all dyes the last occupied state corresponds to a state localized on the molecule which is placed within the cluster band gap, but near the edge of the conduction band. However, regarding to the unoccupied states, the picture is rather different for all dyes. While the dye size increases, the first virtual state with contribution of the dye is located at a lower energy. This state appears well into the conduction band for catechol and 2,3-naphthalenediol (4.0 and 3.0 eV above the Fermi level) and nearer the conduction band lower edge for alizarin, C343, and NKX-2311 (1.6, 1.4, and 1.0 eV above the Fermi level, respectively).

For NKX-2311 the first virtual state localized on the molecule is placed close to the conduction band lower edge, 1.0 eV above the Fermi level. All states below this level are completely localized on the semiconductor without any contribution from the dye, showing weak electronic coupling between dye and TiO_2, and this fact favors excited state electron injection, i.e., the indirect mechanism for electron injection.

In 2,3-naphthalenediol and catechol DOS, the first state with high contribution of the dye appears in the diagram placed well into the conduction band. Like in adsorbed NKX-2311 DOS, the first virtual states are completely localized on the surface. Nevertheless, all states above 0.5 eV have a considerable contribution from the dye molecule. A strong electronic coupling exists in this case, which enforces the direct electron transfer mechanism. For catechol and 2,3-naphthalenediol there is a large number of acceptor states, localized on the TiO_2 but with significant contribution of the dye, located between the last occupied state and the first unoccupied state mainly localized on the dye (that

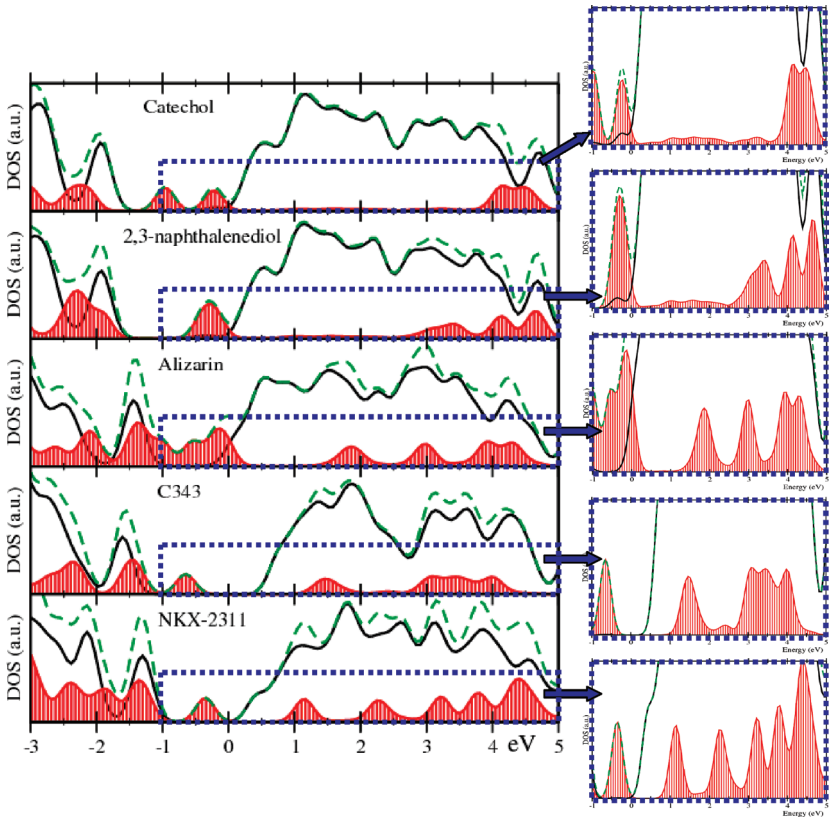

Figure 10. Partial and total density of states for the five dyes adsorbed on $(TiO_2)_9$. Fermi level has been set as the zero energy. The lack full line corresponds to TiO_2 partial DOS, the red line corresponds to dye partial DOS, and the green dashed line corresponds to total DOS. In the right panel, the energy zone between −1 and 5 eV has been zoomed in on.

corresponds to the excited state of the free dye), and these states are responsible for the direct electron injection and for the new band in the spectrum after the adsorption.

Adsorbed alizarin and C343 DOS also present an intermediate behavior. The first virtual state localized on the molecule is placed 1.6 eV above the Fermi level for alizarin and 1.4 eV for C343. Below this energy values, some states with dye contribution appear in adsorbed alizarin DOS, while there are not states localized in the dye in C343 DOS. It is worth noting that alizarin and C343 adsorb to the surface through a different anchor group. Alizarin binds to the surface through two hydroxyl groups, like catechol and 2,3-naphthalenediol, while C343 binds to the surface through a carboxylic group, like NKX-2311.

The electronic coupling between semiconductor conduction band and dye molecule strongly influences the electron injection mechanism. The direct mechanism requires a strong electronic coupling, while weak electronic coupling favors the indirect mechanism. For this reason, to theoretically determine or analyze the type of injection mechanism for a particular dye, it is necessary to include the semiconductor in the model. Moreover, the model size should be large enough to reproduce well the electronic structure of adsorbed dyes. Nevertheless, and due to the high cost of this kind of calculation, only a small number of DSSC sensitizers have been studied employing an adequate model (i.e., including a cluster of considerable size).

4. CONCLUSIONS

The electronic structure and the optical response of five organic dyes, free and bound to TiO_2, have been analyzed using time-dependent density functional theory (TD-DFT) performing calculations both in real time and frequency domains. For all cases, the simulated spectra agree well with the experimental ones. Because of their different geometries and electronic structures, these dyes present important differences as sensitizers, and they present different mechanisms for electronic injection into the semiconductor conduction band. This fact is reflected in the electronic absorption spectra of adsorbed dyes.

From the analysis we conclude that for adsorbed NKX-2311, the photoexcitation occurs toward an orbital mainly localized on the molecule that is not far from the edge of the semiconductor conduction band. This orbital is very similar to the LUMO in the free dye. The red-shift in the electronic spectrum after adsorption arises from a relative stabilization of the destiny orbital as a consequence of hybridization. In contrast, for catechol and 2,3-naphthalenediol adsorbed systems the first virtual orbital mostly localized on the dye appears well into the semiconductor conduction band. In consequence, there are a large number of acceptor orbitals mainly localized on the cluster. Most of these orbitals are formed via interaction of d_{z^2} orbitals of Ti atom closest to the dye molecule and p orbitals of the dye oxygens. A new band appears in the spectrum, which corresponds to a photoexcitation from states fully localized on the dye to states mainly localized on the cluster but with appreciable dye contribution. NKX-2311 and catechol have limit behaviors. Nevertheless, intermediate behaviors are possible. As we move in the sequence catechol, 2,3-naphthalenediol, C343, alizarin, and NKX-2311, we pass progressively from a purely direct injection mechanism to a purely indirect injection mechanism. Alizarin

and C343 represent the intermediate behavior in which both injections regimes are present. The presence of both mechanisms could lead to the observation of different injection rates.

The electronic coupling between semiconductor conduction band and dye molecule strongly influences the electron injection mechanism. The direct mechanism requires a strong electronic coupling, while weak electronic coupling favors the indirect mechanism. To theoretically determine or analyze the kind of injection mechanism for a particular dye, it is necessary to include the effect of the semiconductor explicitly in the model. In addition, the cluster size should be large enough to reproduce well the electronic structure of adsorbed dyes.

AUTHOR INFORMATION

Corresponding Author
*E-mail: rociosa@us.es.

ACKNOWLEDGMENT

This work was funded by the Spanish Ministerio de Ciencia e Innovación, MICINN, projects MAT2008-4918 and CSD2008-0023. R.S.A. thanks the Junta de Andalucía for a predoctoral grant (P08-FQM-3661 and EXC/2005/FQM-1126). Part of the calculations has been carried out at the Barcelona Supercomputing Center, Centro Nacional de Supercomputación, Spain.

REFERENCES

(1) Grätzel, M. *Nature* **2001**, *414*, 338.
(2) Duncan, W. R.; Prezhdo, O. V. *Annu. Rev. Phys. Chem.* **2007**, *58*, 143.
(3) Ning, Z.; Fu, Y.; Tian, H. *Energy Environ.* **2010**, *3*, 1170.
(4) Mishra, A.; Fischer, M. K. R.; Bäulere, P. *Angew. Chem., Int. Ed.* **2009**, *48*, 2474.
(5) Ooyama, Y.; Harima, Y. *Eur. J. Org. Chem.* **2009**, 2903.
(6) Duncan, W. R.; Stier, W. M.; Prezhdo, O. V. *J. Am. Chem. Soc.* **2005**, *127*, 7941.
(7) Nawrocka, A.; Krawczyk, S. *J. Phys. Chem. C* **2008**, *112*, 10233.
(8) Macyk, W.; Szacilowski, K.; Stochel, G.; Buchalska, M.; Kuncewicz, J; Labuz, P. *Coord. Chem. Rev.* **2010**, *254*, 2687.
(9) De Angelis, F. *Chem. Phys. Lett.* **2010**, *493*, 323.
(10) Duncan, W. R.; Prezhdo, O. V. *J. Phys. Chem. B* **2005**, *109*, 365.
(11) Duncan, W. R.; Craig, C. F.; Prezhdo, O. V. *J. Am. Chem. Soc.* **2007**, *129*, 8528.
(12) Duncan, W. R.; Prezhdo, O. V. *J. Am. Chem. Soc.* **2008**, *130*, 9756.
(13) Kaniyankandy, S.; Verma, S.; Mondal, J. A.; Palit, D. K.; Ghosh, H. N. *J. Phys. Chem. C* **2009**, *113*, 3593.
(14) Huber, R.; Moser, J. E.; Grätzel, M.; Wachtveitl, J. *J. Phys. Chem. B* **2002**, *106*, 6494.
(15) Huber, R.; Spörlein, S; Moser, J. E.; Grätzel, M.; Wachtveitl, J. *J. Phys. Chem. B* **2000**, *104*, 8995.
(16) Liu., Y.; Dapad, J. I.; Zimdars, D.; Eisenthal, K. B. *J. Phys.Chem. B* **1999**, *103*, 2480.
(17) Wang, Y.; Hang, K.; Anderson, N. A.; Lian, T. *J. Phys. Chem. B* **2003**, *107*, 9434.
(18) Moser, J.; Punchihewa, S.; Infelta, P. P.; Grätzel, M. *Langmuir* **1991**, *7*, 3012.
(19) Rodríguez, R.; Blesa, M. A.; Regazzoni, A. E. *J. Colloid Interface Sci.* **1996**, *177*, 122.
(20) Tae, E. L.; Lee, S. H.; Lee, J. K.; Yoo, S. S.; Kang, E. J.; Yoon, K. B. *J.Phys. Chem. B* **2005**, *109*, 22513.
(21) Nazeeruddin, M. K.; De Angelis, F.; Fantacci, S.; Selloni, A.; Viscardi, G.; Liska, P.; Ito, S.; Takeru, B.; Grätzel, M. *J. Am. Chem. Soc.* **2005**, *127*, 16835.
(22) Kondov, I.; Wang, H.; Thoss, M. *Int. J. Quantum Chem.* **2006**, *106*, 1291.
(23) Guo, Z.; Liang, W. Z.; Zhao, Y.; Chen, G. H. *J. Phys. Chem. C* **2008**, *112*, 16655.
(24) Sánchez-de-Armas, R.; Oviedo, J; San Miguel, M. A.; Ordejón, P.; Pruneda, M.; Sanz, J. F. *J. Chem. Theory Comput.* **2010**, *6*, 2856.
(25) Sánchez-de-Armas, R.; San-Miguel, M. A.; Oviedo, J.; Márquez, A.; Sanz, J. F. *Phys. Chem. Chem. Phys.* **2011**, *13*, 1506.
(26) Rhem, J. M.; McLendon, G. L.; Nagasawa, Y.; Yoshihara, K.; Moser, J.; Grätzel, M. *J. Phys. Chem.* **1996**, *100*, 9577.
(27) Ghosh, H. N.; Asbury, J. B.; Lian, T. *J. Phys. Chem. B* **1998**, *102*, 6482.
(28) Frontiera, R. R.; Dasgupta, J.; Mathies, A. *J. Am. Chem. Soc.* **2009**, *131*, 15630.
(29) Hara, K.; Sayama, K.; Ohga, Y.; Shinpo, A.; Suga, S.; Arakawa, H. *Chem. Commun.* **2001**, 569.
(30) Hara, K.; Sato, T.; Katoh, R.; Furube, A.; Ohga, Y.; Shinpo, A.; Suga, S.; Sayama, K.; Sugihara, H.; Arakawa, H. *J. Phys. Chem. B* **2003**, *107*, 597.
(31) Perdew, J. P.; Burke, K. *Phys. Rev. Let.* **1996**, *77*, 3865.
(32) Troullier, N.; Martins, J. L. *Phys. Rev. B* **1991**, *43*, 1993.
(33) Kleinman, L.; Bylander, D. M. *Phys. Rev. Lett.* **1982**, *48*, 1425.
(34) Artacho, E.; Sánchez-Portal, D.; Ordejón, P.; García, A.; Soler, J. M. *Int. J. Quantum Chem. Status Solidi B* **1999**, *215*, 809.
(35) Junquera, J.; Paz, O.; Sanchez-Portal, D.; Artacho, E. *Phys. Rev. B* **2001**, *64*, 235111.
(36) Anglada, E.; Soler, J. M.; Junquera, J.; Artacho, E. *Phys. Rev. B* **2002**, *66*, 205101.
(37) Soler, J. M.; Artacho, E.; Gale, J. D.; García, A.; Junquera, J.; Ordejón, P.; Sánchez-Portal, D. J. *Phys. Condens. Matter* **2002**, *14*, 2745.
(38) Sánchez-Portal, D.; Ordejón, P.; Artacho, E.; Soler, J. M. *Int. J. Quantum Chem.* **1997**, *67*, 453.
(39) Tsolakidis, A.; Sánchez-Portal, D.; M. Martin, R. *Phys. Rev. B* **2002**, *66*, 235416.
(40) Frisch, M. J.; Trucks, G. W.; Schlegel, H. B.; Scuseria, G. E. ; Rob, M. A. ; Cheeseman, J. R. ; Montgomery, J. A., Jr.; Vreven, T.; Kudin, K. N.; Burant, J. C.; Millam, J. M.; Iyengar, S. S.; Tomasi, J. ; Barone, V.; Mennucci, B.; Cossi, M.; Scalmani, G.; Rega, N.; Petersson, G. A.; Nakatsuji, H.; Hada, M.; Ehara, M.; Toyota, K.; Fukuda, R.; Hasegawa, J.; Ishida, M.; Nakajima, T.; Honda, Y.; Kitao, O.; Nakai, H.; Klene, M.; Li, X.; Knox, J. E.; Hratchian, H. P.; Cross, J. B.; Bakken, V.; Adamo, C.; Jaramillo, J.; Gomperts, R.; Stratmann, R. E.; Yazyev, O.; Austin, A. J.; Cammi, R.; Pomelli, C.; Ochterski, J. W.; Ayala, P. Y.; Morokuma, K.; Voth, G. A.; Salvador, P.; Dannenberg, J. J.; Zakrzewski, V. G.; Dapprich, S.; Daniels, A. D.; Strain, M. C.; Farkas, O.; Malick, D. K.; Rabuck, A. D.; Raghavachari, K.; Foresman, J. B.; Ortiz, J. V.; Cui, Q.; Baboul, A. G.; Clifford, S.; Cioslowski, J.; Stefanov, B. B.; Liu, G.; Liashenko, A.; Piskorz, P.; Komaromi, I.; Martin, R. L.; Fox, D. J.; Keith, T.; Al-Laham, M. A. ; Peng, C. Y.; Nanayakkara, A.; Challacombe, M.; Gill, P. M. W.; Johnson, B.; Chen, W.; Wong, M. W.; Gonzalez, C.; Pople, J. A. *Gaussian 03*; Gaussian, Inc.: Wallingford, CT, 2003.
(41) Qu, Z.; Kroes, G. *J. Phys. Chem. B* **2006**, *110*, 8998.
(42) Hamad, S.; Catlow, C. R. A.; Woodley, S. M.; Lago, S.; Mejías, J. A. *J. Phys. Chem. B* **2005**, *109*, 15741.
(43) Wang, Z.; Hara, K.; Dan-oh, Y.; Kasada, C.; Shinpo, A.; Suga, S.; Arakawa, H.; Sugihara, H. *J. Phys. Chem. B* **2005**, *109*, 3907.